



**HAL**  
open science

# A wave based method for computing high-frequency radiation

Denis Duhamel

► **To cite this version:**

Denis Duhamel. A wave based method for computing high-frequency radiation. EUROODYN 2011, Jul 2011, Leuven, Belgium. pp.634-641. hal-00668520

**HAL Id: hal-00668520**

**<https://hal.science/hal-00668520>**

Submitted on 9 Feb 2012

**HAL** is a multi-disciplinary open access archive for the deposit and dissemination of scientific research documents, whether they are published or not. The documents may come from teaching and research institutions in France or abroad, or from public or private research centers.

L'archive ouverte pluridisciplinaire **HAL**, est destinée au dépôt et à la diffusion de documents scientifiques de niveau recherche, publiés ou non, émanant des établissements d'enseignement et de recherche français ou étrangers, des laboratoires publics ou privés.

# A wave based method for computing high-frequency radiation

Denis Duhamel

Université Paris-Est, Laboratoire Navier, ENPC/IFSTTAR/CNRS

6 et 8 Avenue Blaise Pascal, Cité Descartes, Champs sur Marne, 77455 Marne la Vallée, cedex 2, France  
email : denis.duhamel@enpc.fr

**ABSTRACT:** The calculation of high-frequency wave radiations in exterior domains by finite element methods can lead to large computations. Boundary conditions have to be applied on the surface of the radiating body or on a truncated domain to approximate the behaviour of an infinite domain. In this paper, a different waveguide approach is proposed for computing wave radiation. Propagation constants and wave modes are computed in a small rib around the radiating body for different frequencies. It is shown that the solutions on the boundary of the radiating body and in the exterior domain can be determined efficiently from this set of waves. The method allows an efficient computation of radiation and scattering solutions by limiting the discretization to a very small part of the exterior domain. The error on the boundary condition can be controlled and the solution converges to the exact solution by using a sufficient number of waves. It is shown that the condition is more efficient for high frequencies and can be complementary of the usual approaches involving simple finite or boundary elements. Analytical and numerical examples are computed to show the accuracy of the method.

**KEY WORDS:** Wave propagation; radiation; scattering; high frequency; infinite domain; boundary condition; wave finite element.

## 1 INTRODUCTION

Many approaches have been used in the past for computing the solutions of wave problems in unbounded media. They can be mainly classified into two groups : the domain methods for which a substantial part of the exterior domain is meshed and the surface methods for which only the surface of the domain is meshed. In the domain methods the exterior domain is truncated at some distance where local or global boundary conditions are imposed at this artificial boundary. Boundary conditions at finite distance must simulate as closely as possible the exact radiation condition at infinity and, to this aim, various methods have been proposed, see [1], [2], [3], [4], [5] among many papers on this subject. An alternative method is to use boundary elements as described in numerous classical textbooks like [6], [7], [8]. It consists in solving an equation on the boundary of the domain only and so the radiation conditions are taken into account analytically. However, the final problem usually involves full matrices which are also often non symmetrical. So this method can lead to heavy computations when the number of degrees of freedom increases, for instance for high frequencies. To try to overcome this problem, the fast multipole method was developed by many authors like [9], [10], [11]. In this approach the Green's function of the problem is expanded in multipole by grouping the computation of the interactions between far-away basis functions. Using a multilevel approach, the number of operations can be reduced to the order of  $O(N \log N)$  where  $N$  is the number of degrees of freedom on the boundary. This considerably increases the potential of boundary element methods but this needs complicated programming and must be adapted for different Green's functions.

In this paper, we propose a quite different approach consisting in the description of the propagation in exterior domains using

variants of methods originally developed to describe waveguide structures. Classically these structures are uniform or periodic along an axis, which is not the case here, so this paper describes how to adapt these classical methods for exterior wave propagation problems. The motivation is that such waveguides have been the topic of much research and efficient descriptions of wave propagation in these structures have been proposed both theoretically and numerically.

One can find analytical or finite element models of waveguide and people are generally interested by the computation of wave propagations and dispersion curves or by the determination of the frequency response functions. For general waveguides with a complex cross-section, the displacements in the cross-section can be described by the finite element method while the variation along the axis of symmetry is expressed as a wave function. Following these ideas, [12], [13], [14], [15] developed the spectral finite element approach. This leads to efficient computations of dispersion relations and transfer functions.

More general waveguides can be studied by considering periodic structures. Numerous works provided interesting theoretical insights in the behaviour of these structures, see for instance the work of [16] and the review paper by [17]. Mead also presented a general theory for wave propagation in periodic systems in [18], [19], [20]. He showed that the solution can be decomposed into an equal number of positive and negative-going waves. The approach is mainly based on Floquet's principle or the transfer matrix and the objective is to compute propagation constants relating the forces and displacements on the two sides of a single period and the waves associated to these constants. For complex structures FE models are used for the computation of the propagation constants and waves. The final objective is to compute dispersion relations to use them in energetic methods or to find transfer functions in the

waveguide, see [21], [22], [23], [24], [25]. In [26] the general dynamic stiffness matrix for a periodic structure was found from the propagation constants and waves.

The aim of this paper is to link these two, apparently quite different, subjects. Here, a waveguide method, based on ideas related to wave finite elements as described in [5], [21], [26], [27], is used to compute the solution in the exterior domain using functions defined on a small rib around the radiating body. Propagation constants and wave modes are introduced. It is shown how the solution in the exterior domain can be computed for various frequencies using a simple relation between domains of homothetic sizes and their propagating modes.

This paper is divided into three sections and is outlined as follows. In section two, waves are computed in a layer around the radiating body and relations between layers are given. In section three, numerical examples are given to test the efficiency of the method before the conclusion.

## 2 WAVEGUIDE APPROACH

### 2.1 Introduction

The problem is illustrated in figure 1, where harmonic waves propagate at the exterior of a body  $\Omega$ . Consider a surface  $\Gamma$  in the exterior domain around the body, this surface is obtained from  $\partial\Omega$  by a homothety of factor  $\alpha$ . Only convex bodies are studied here.

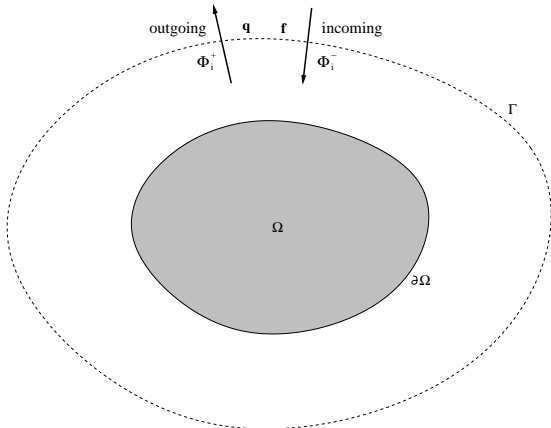


Figure 1. Exterior domain with incoming and outgoing waves.

We define the state vector  $\mathbf{s}$  on  $\Gamma$  as the vector made of the displacement  $\mathbf{q}$  and a term proportional to the force  $\frac{1}{i\omega}\mathbf{f}$ . Both terms are multiplied by  $\alpha^d$  where  $d = (n - 1)/2$  and  $n$  is the space dimension. The  $\alpha^d$  term is introduced to allow the conservation of the scalar product at different distances from the surface as will be seen later. We suppose that a solution in the exterior domain can be decomposed as a sum of incoming and outgoing waves, with outgoing waves of amplitudes  $a_i^+$  on a basis  $\Phi_i^+$  and incoming waves of amplitudes  $a_i^-$  on a basis  $\Phi_i^-$ . So we get, for  $\mathbf{x} \in \Gamma$

$$\mathbf{s}(\mathbf{x}) = \begin{pmatrix} \alpha^d \mathbf{q}(\mathbf{x}) \\ \alpha^d \mathbf{f}(\mathbf{x}) \end{pmatrix} = \sum_{i=1}^{i=N} a_i^+ \Phi_i^+(\mathbf{x}) + \sum_{i=1}^{i=N} a_i^- \Phi_i^-(\mathbf{x}) \quad (1)$$

It is supposed that the waves  $\Phi_i^+$  are associated with energy going towards the exterior while waves  $\Phi_i^-$  are associated with

energy converging towards the body. The solution will be purely radiating if  $a_i^- = 0$  for all  $i$ . In the following, the objective is to compute the basis  $\Phi_i^+$  and  $\Phi_i^-$ , at various frequencies and to define boundary conditions on the surface of  $\Omega$  leading to outgoing waves only.

### 2.2 Solutions on different surfaces

Consider now the situation of figure 2, where different surfaces are located at homothetic distances from the reference surface  $S_0 = \partial\Omega$  taken as the surface of the body.

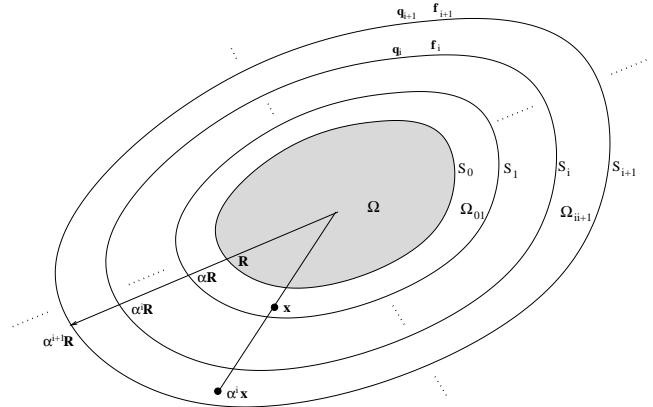


Figure 2. Exterior domain divided into zones of proportional sizes.

For instance the surface  $S_i$  is defined from the surface  $S_0$  by a homothety on the distance from origin such that  $r_i = \alpha_i r_0$  where  $r_0$  is the distance to the origin of a point on  $S_0$ ,  $r_i$  is the corresponding point on  $S_i$  and  $\alpha_i$  is constant on the surface  $S_i$ . Functions on the surface  $S_i$  are linked to functions on  $S_0$  by

$$\begin{aligned} S_0 &\longrightarrow S_i \\ P_i(r_0) &\longmapsto p_i(r_i) = \frac{1}{\alpha_i^d} P_i\left(\frac{r_i}{\alpha_i}\right) \end{aligned} \quad (2)$$

The constant  $d$  is chosen to preserve the scalar product between the different surfaces. We can check that

$$\begin{aligned} \int_{S_i} p_i(r_i) q_i(r_i) ds_i &= \int_{S_0} P_i\left(\frac{r_i}{\alpha_i}\right) Q_i\left(\frac{r_i}{\alpha_i}\right) ds_0 \\ &= \int_{S_0} P_i(r_0) Q_i(r_0) ds_0 \end{aligned} \quad (3)$$

meaning that the scalar product is preserved by the transformation.

Consider now the eigenvalue problem in the annular domain  $\Omega_{ie}$  between the surfaces  $S_i$  and  $S_e$  (see figure 2) in which one associates the displacements and the forces on surfaces  $S_i$  and  $S_e$  as

$$\begin{cases} L(\mathbf{q}) + \omega^2 \mathbf{q} = 0 & \text{in } \Omega_{ie} \\ \alpha_e^d \mathbf{q}_e(r_e) = \lambda \alpha_i^d \mathbf{q}_i(r_i) \\ \alpha_e^d \mathbf{f}_e(r_e) = \lambda \alpha_i^d \mathbf{f}_i(r_i) \end{cases} \quad (4)$$

where  $L$  is a second order partial differential operator (for instance  $\Delta$  or the linear elasticity operator). The relations on the boundaries can also be written as

$$\begin{cases} \mathbf{Q}_e(r_0) = \lambda \mathbf{Q}_i(r_0), & \text{on } S_0 \\ \mathbf{F}_e(r_0) = \lambda \mathbf{F}_i(r_0), & \text{on } S_0 \end{cases} \quad (5)$$

### 2.3 Behaviour of a layer

A layer defined as the domain  $\Omega_{ie}$ , between surfaces  $S_i$  and  $S_e$  is described by a finite element model. It is supposed that the inner and outer surfaces have sizes proportional to the surfaces of the body  $S_0$ , that means that points on these surfaces are given by  $\mathbf{x}_i = \alpha_i \mathbf{x}_0$  and  $\mathbf{x}_e = \alpha_e \mathbf{x}_0$  where  $\alpha_i$  and  $\alpha_e$  are constants on their respective surfaces. A layer can be meshed with an arbitrary number of elements using the full possibilities of usual finite element software. The discrete dynamic behaviour of a layer obtained from a finite element model at a circular frequency  $\omega$  is given by

$$(\mathbf{K} - \omega^2 \mathbf{M})\mathbf{Q} = \mathbf{F} \quad (6)$$

where  $\mathbf{K}$  and  $\mathbf{M}$  are the stiffness and mass matrices respectively,  $\mathbf{F}$  is the loading vector and  $\mathbf{Q}$  the vector of the degrees of freedom. The stiffness and mass matrices could be obtained from any commercial finite element software and so this allows the consideration of layers with complex structures. The sizes of these matrices depends on the number of elements used to mesh the layer and can be arbitrarily increased for a better precision of the results. Introducing the dynamic stiffness matrix of the layer  $\mathbf{D}^L = \mathbf{K} - \omega^2 \mathbf{M}$ , decomposing into boundary (B) and interior (I) degrees of freedom, and assuming that there are no external forces on the interior nodes, results in the following relation

$$\begin{bmatrix} \mathbf{D}_{BB}^L & \mathbf{D}_{BI}^L \\ \mathbf{D}_{IB}^L & \mathbf{D}_{II}^L \end{bmatrix} \begin{bmatrix} \mathbf{Q}_B \\ \mathbf{Q}_I \end{bmatrix} = \begin{bmatrix} \mathbf{F}_B \\ \mathbf{0} \end{bmatrix} \quad (7)$$

The assumption that there are no forces on the interior degrees of freedom is satisfied for free waves inside the structure for which the forces on a layer are only produced by boundary forces from the adjacent layers. The interior degrees of freedom can thus be eliminated to get

$$\mathbf{F}_B = (\mathbf{D}_{BB}^L - \mathbf{D}_{BI}^L (\mathbf{D}_{II}^L)^{-1} \mathbf{D}_{IB}^L) \mathbf{Q}_B \quad (8)$$

Dropping the  $B$  index, this relation is written in the sequel as

$$\mathbf{F} = \mathbf{D}^L \mathbf{Q} \quad (9)$$

and only boundary degrees of freedom will be considered now. Separating the dofs into the inner ( $i$ ) and outer ( $e$ ) boundaries leads to

$$\begin{bmatrix} \mathbf{D}_{ii}^L & \mathbf{D}_{ie}^L \\ \mathbf{D}_{ei}^L & \mathbf{D}_{ee}^L \end{bmatrix} \begin{bmatrix} \mathbf{Q}_i \\ \mathbf{Q}_e \end{bmatrix} = \begin{bmatrix} \mathbf{F}_i \\ \mathbf{F}_e \end{bmatrix} \quad (10)$$

By symmetry of the stiffness and mass matrices, the dynamic stiffness matrix is also symmetric, which leads to  ${}^t \mathbf{D}_{ii}^L = \mathbf{D}_{ii}^L$ ,  ${}^t \mathbf{D}_{ee}^L = \mathbf{D}_{ee}^L$  and  ${}^t \mathbf{D}_{ie}^L = \mathbf{D}_{ei}^L$ , where the superscript  $t$  indicates the transpose.

Instead of working with the current variables defined on surfaces  $S_i$  and  $S_e$ , we will work with reference variables defined on the reference surface  $S_0$  as described in relation (2) such that

$$\begin{aligned} \mathbf{Q}_i &= \alpha_i^d \mathbf{q}_i \\ \mathbf{Q}_e &= \alpha_e^d \mathbf{q}_e \\ \mathbf{F}_i &= i\omega \alpha_i^{-d} \mathbf{f}_i \\ \mathbf{F}_e &= i\omega \alpha_e^{-d} \mathbf{f}_e \end{aligned} \quad (11)$$

This change of variable is introduced to preserve the scalar product between functions defined on  $S_0$ ,  $S_i$  and  $S_e$ . The

relations in (11) should be identical in terms of displacement and force density. However, the nodal values of the force in the finite element model are obtained through an integration over surface elements and so already include an  $\alpha^{2d}$  contribution. This leads finally to the  $\alpha_e^{-d}$  term in the relation involving the nodal force values. The term  $i\omega$  is introduced as a normalisation of the scale between homothetic layers as will be seen later. Thus, the behaviour of a layer is now given by

$$\begin{bmatrix} \mathbf{f}_i \\ \mathbf{f}_e \end{bmatrix} = \frac{1}{i\omega} \begin{bmatrix} \alpha_i^{2d} \mathbf{D}_{ii}^L & \alpha_i^d \alpha_e^d \mathbf{D}_{ie}^L \\ \alpha_i^d \alpha_e^d \mathbf{D}_{ei}^L & \alpha_e^{2d} \mathbf{D}_{ee}^L \end{bmatrix} \begin{bmatrix} \mathbf{q}_i \\ \mathbf{q}_e \end{bmatrix} = \begin{bmatrix} \mathbf{D}_{ii} & \mathbf{D}_{ie} \\ \mathbf{D}_{ei} & \mathbf{D}_{ee} \end{bmatrix} \begin{bmatrix} \mathbf{q}_i \\ \mathbf{q}_e \end{bmatrix} \quad (12)$$

### 2.4 Eigenvalue problem

In terms of the variables  $\mathbf{f}$  and  $\mathbf{q}$ , free wave propagation is described by the discrete eigenproblem

$$\begin{cases} \mathbf{q}_e = \lambda \mathbf{q}_i \\ \mathbf{f}_e + \lambda \mathbf{f}_i = 0 \end{cases} \quad (13)$$

where  $\lambda$  is a propagation constant between the inner and outer boundaries of the domain  $\Omega_{ie}$ . Combining these two relations with relation (12) yields

$$\left( \mathbf{D}_{ii} + \mathbf{D}_{ee} + \lambda \mathbf{D}_{ie} + \frac{1}{\lambda} \mathbf{D}_{ei} \right) \mathbf{q}_i = 0 \quad (14)$$

The eigenvector  $\mathbf{q}_i$  is thus the solution of a quadratic eigenvalue problem. Taking the transpose of equation (14) shows that  $\mathbf{q}_i$  is both a right-eigenvector associated with the eigenvalue  $\lambda$  and a left-eigenvector associated with the eigenvalue  $1/\lambda$ . Since the left and right eigenproblems have identical eigenvalues, it follows that if  $\lambda$  is an eigenvalue then so, too, is  $1/\lambda$ . These represent a pair of positive- and negative-going waves.

Introducing the transfer matrix

$$\mathbf{T} = \begin{bmatrix} -\mathbf{D}_{ie}^{-1} \mathbf{D}_{ii} & \mathbf{D}_{ie}^{-1} \\ -\mathbf{D}_{ei} + \mathbf{D}_{ee} \mathbf{D}_{ie}^{-1} \mathbf{D}_{ii} & -\mathbf{D}_{ee} \mathbf{D}_{ie}^{-1} \end{bmatrix} \quad (15)$$

such that

$$\mathbf{T} \begin{bmatrix} \mathbf{q}_i \\ \mathbf{f}_i \end{bmatrix} = \begin{bmatrix} \mathbf{q}_e \\ \mathbf{f}_e \end{bmatrix} \quad (16)$$

This matrix has a right eigenvector for the eigenvalue  $\lambda_i$  given by

$$\Phi_i = \begin{bmatrix} \mathbf{q}(\lambda_i) \\ (\mathbf{D}_{ii} + \lambda_i \mathbf{D}_{ie}) \mathbf{q}(\lambda_i) \end{bmatrix} \quad (17)$$

and a left eigenvector associated with  $\lambda_i$  given by

$$\Psi_i = \left[ {}^t \mathbf{q} \left( \frac{1}{\lambda_i} \right) (\mathbf{D}_{ee} + \lambda_i \mathbf{D}_{ie}) \quad {}^t \mathbf{q} \left( \frac{1}{\lambda_i} \right) \right] \quad (18)$$

where  $\mathbf{q}(\lambda_i)$  and  $\mathbf{q}(\frac{1}{\lambda_i})$  are the eigenvectors of (14) associated to the eigenvalues  $\lambda_i$  and  $1/\lambda_i$  respectively. Orthogonality properties can be obtained from these relationships. Considering

$$\mathbf{T} \Phi_j = \lambda_j \Phi_j \quad (19)$$

$$\Psi_i \mathbf{T} = \lambda_i \Psi_i \quad (20)$$

which leads to

$$\Psi_i \mathbf{T} \Phi_j = \lambda_j \Psi_i \Phi_j = \lambda_i \Psi_i \Phi_j \quad (21)$$

This quantity must equal zero if  $\lambda_i \neq \lambda_j$ , so, the left and right eigenvectors are such that

$$\Psi_i \Phi_j = d_i \delta_{ij} \quad (22)$$

where  $d_i$  is some constant. A normalisation of the eigenvectors could be chosen such that  $d_i = 1$ .

### 2.5 Wave decomposition in a layer

From the precedent section, it is clear that the  $2N$  eigenvalues of equation (14) can be split into two sets of  $N$  eigenvalues and eigenvectors which are denoted by  $(\lambda_i, \Phi_i^+)$  and  $(1/\lambda_i, \Phi_i^-)$ , with the first set such that  $|\lambda_i| \leq 1$ . In the case  $|\lambda_i| = 1$ , the first set must contain the waves propagating in the positive direction, which are such that  $\text{Re}\{(i\omega)^2 \mathbf{q}_i^H \mathbf{f}_i\} < 0$ . The inverse eigenvalue  $1/\lambda_i$ , in the second set, is associated with the waves such that  $\text{Re}\{(i\omega)^2 \mathbf{q}_i^H \mathbf{f}_i\} > 0$ .

These waves are now used as a basis in a layer. The inner state vector is given by the following sum of positive and negative-going waves with respective amplitudes  $a_i^+$  and  $a_i^-$

$$\mathbf{x}_i = \begin{bmatrix} \mathbf{q}_i \\ \mathbf{f}_i \end{bmatrix} = \sum_{i=1}^{i=N} (a_i^+ \Phi_i^+ + a_i^- \Phi_i^-) \quad (23)$$

In the same way, the outer state vector is given by

$$\mathbf{x}_e = \begin{bmatrix} \mathbf{q}_e \\ \mathbf{f}_e \end{bmatrix} = \sum_{i=1}^{i=N} (\lambda_i a_i^+ \Phi_i^+ + 1/\lambda_i a_i^- \Phi_i^-) \quad (24)$$

### 2.6 Solutions in homothetic zones

Consider now the situation of figure 2, where the body  $\Omega$  is surrounded by an infinite number of layers of homothetic sizes such that the positions in zones  $\Omega_{ii+1}$  and  $\Omega_{i+1i+2}$  are related by  $\mathbf{x}^{i+1} = \alpha \mathbf{x}^i$ , where  $\alpha$  is a constant parameter. Using the results of the precedent section, eigenvalues and eigenvectors are computed in the domain  $\Omega_{ii+1}$  between surfaces  $S_i$  and  $S_{i+1}$ . This eigenvalue problem is

$$\begin{cases} L(\mathbf{q}) + \omega^2 \mathbf{q} = 0 & \text{in } \Omega_{ii+1} \\ \alpha^{(i+1)d} \mathbf{q}_{i+1} = \lambda \alpha^{id} \mathbf{q}_i \\ \alpha^{(i+1)d} \mathbf{f}_{i+1} = \lambda \alpha^{id} \mathbf{f}_i \end{cases} \quad (25)$$

where  $\mathbf{q}_i$  and  $\mathbf{q}_{i+1}$  are the displacements on surfaces  $S_i$  and  $S_{i+1}$  respectively, while  $\mathbf{f}_i$  and  $\mathbf{f}_{i+1}$  are the normal forces (divided by  $i\omega$ ). The eigenproblem in the following layer,  $\Omega_{i+1i+2}$  is

$$\begin{cases} L(\mathbf{q}) + \omega^2 \mathbf{q} = 0 & \text{in } \Omega_{i+1i+2} \\ \alpha^{(i+2)d} \mathbf{q}_{i+2} = \lambda \alpha^{(i+1)d} \mathbf{q}_{i+1} \\ \alpha^{(i+2)d} \mathbf{f}_{i+2} = \lambda \alpha^{(i+1)d} \mathbf{f}_{i+1} \end{cases} \quad (26)$$

This is the same eigenvalue problem as for zone  $\Omega_{ii+1}$  but for the frequency  $\alpha\omega$ . More precisely, one has an eigenvector in the domain  $\Omega_{i+1i+2}$  from an eigenvector in the domain  $\Omega_{ii+1}$  by

$$\begin{aligned} \Phi_j^{i+1}(\alpha \mathbf{x}, \omega) &= \Phi_j^i(\mathbf{x}, \alpha\omega) \\ \lambda_j^{i+1}(\omega) &= \lambda_j^i(\alpha\omega) \end{aligned} \quad (27)$$

where  $\Phi_j^i(\mathbf{x}, \omega)$  denotes the eigenvectors (the value of the solution on the inner surface  $S_i$ ) and  $\lambda_j^i(\omega)$  the eigenvalues of

zone  $\Omega_{ii+1}$  at the frequency  $\omega$ . Finally, the eigenvectors and eigenvalues in any domain can be computed from those of the first domain by

$$\begin{aligned} \Phi_j^i(\alpha^i \mathbf{x}, \omega) &= \Phi_j^0(\mathbf{x}, \alpha^i \omega) \\ \lambda_j^i(\omega) &= \lambda_j^0(\alpha^i \omega) \end{aligned} \quad (28)$$

The solution in the exterior domain around  $\Omega$  can be decomposed on these eigenvectors. Defining the state vector on the surface  $S_i$  by  $\mathbf{s}^i = {}^t(\alpha^{id} \mathbf{q}_i, \alpha^{id} \mathbf{f}_i)$  (with a normal towards the exterior domain), the decomposition of the solution in term of waves with amplitudes  $\mathbf{a}^i$  is given by

$$\mathbf{s}^i = \Phi^i \cdot \mathbf{a}^i = \sum_{j=1}^{j=2N} a_j^i \Phi_j^i \quad (29)$$

where  $\Phi^i$  is the matrix made of the  $\Phi_j^i$  and  $\mathbf{a}^i$  the vector of the  $a_j^i$ . So, between two consecutive layers, one gets

$$\begin{aligned} \mathbf{s}^{i+1} &= \Phi^i \cdot \Lambda^i \cdot \mathbf{a}^i \\ &= \Phi^i \cdot \Lambda^i \cdot \Psi^i \cdot \mathbf{s}^i \\ &= \mathbf{T}^i \cdot \mathbf{s}^i \end{aligned} \quad (30)$$

where the different matrices are defined by

$$\begin{aligned} \Phi^i &= [\Phi_1^i, \dots, \Phi_{2N}^i] \\ \Psi^i &= [\Psi_1^i, \dots, \Psi_{2N}^i] \\ \Lambda^i &= \text{diag}[\lambda_1^i, \dots, \lambda_{2N}^i] \\ \mathbf{T}^i &= \Phi^i \cdot \Lambda^i \cdot \Psi^i \end{aligned} \quad (31)$$

if we retain  $N$  positive-going and  $N$  negative-going waves. From the properties seen previously, one has

$$\begin{aligned} \Phi^i(\omega) &= \Phi^{i-1}(\alpha\omega) = \Phi^0(\alpha^i \omega) \\ \Psi^i(\omega) &= \Psi^{i-1}(\alpha\omega) = \Psi^0(\alpha^i \omega) \\ \Lambda^i(\omega) &= \Lambda^{i-1}(\alpha\omega) = \Lambda^0(\alpha^i \omega) \\ \mathbf{T}^i(\omega) &= \mathbf{T}^{i-1}(\alpha\omega) = \mathbf{T}^0(\alpha^i \omega) \end{aligned} \quad (32)$$

So, for the complete exterior domain until surface  $S_n$ , one has

$$\mathbf{s}^n = \mathbf{T}^{n-1} \dots \mathbf{T}^0 \mathbf{s}^0 = \mathbf{T}^0(\alpha^{n-1} \omega) \mathbf{T}^0(\alpha^{n-2} \omega) \dots \mathbf{T}^0(\omega) \mathbf{s}^0 = \mathbf{T}^{tot} \mathbf{s}^0 \quad (33)$$

Finally, the boundary condition must be such that the amplitudes of the negative going waves are null, meaning that

$$\Psi_j^n(\omega) \mathbf{T}^{tot} \mathbf{s}^0 = 0 \quad (34)$$

for all  $j$  associated to incoming waves. The state vector on surface  $S_0$  is written as

$$\mathbf{s}^0 = \begin{bmatrix} \mathbf{q}_0 \\ \mathbf{f}_0 \end{bmatrix} \quad (35)$$

and the matrix as

$$\Psi^-(\omega) \mathbf{T}^{tot} = [ \mathbf{F}_0 \quad \mathbf{Q}_0 ] \quad (36)$$

where  $\Psi^-(\omega)$  is a matrix made from the left vectors  $\Psi_j^n$  associated to negative-going waves. Finally, the boundary condition can be written as the impedance condition

$$\mathbf{F}_0 \mathbf{q}_0 + \mathbf{Q}_0 \mathbf{f}_0 = 0 \quad (37)$$

This gives the relation on the surface of  $\Omega$  approximating the radiation condition.

### 3 EXAMPLES

To illustrate the precedent approach we consider now three simple examples.

#### 3.1 One-dimensional waveguide

The pressure in a one-dimensional waveguide is solution of

$$p'' + k^2 p = 0 \quad (38)$$

in the domain  $[L, +\infty[$ . The state vector is defined in terms of the variable  $p$  and  $q = \frac{1}{ik} p'$  such that  $\mathbf{s} = {}^t(p \ q)$ . The eigenvalue problem in the interval  $[L, \alpha L]$  is

$$\begin{aligned} p'' + k^2 p &= 0 \\ p(\alpha L) &= \lambda p(L) \\ \frac{1}{ik} p'(\alpha L) &= \frac{1}{ik} \lambda p'(L) \end{aligned} \quad (39)$$

Thus, the solutions of this problem, the eigenvalues and the eigenvectors at point  $L$ , are

$$\begin{aligned} \Phi^+(k) &= \begin{bmatrix} 1 \\ 1 \end{bmatrix} \\ \Psi^+(k) &= \begin{bmatrix} \frac{1}{2} & \frac{1}{2} \end{bmatrix} \\ \lambda^+(k) &= e^{i(\alpha-1)kL} \\ \Phi^-(k) &= \begin{bmatrix} 1 \\ -1 \end{bmatrix} \\ \Psi^-(k) &= \begin{bmatrix} \frac{1}{2} & -\frac{1}{2} \end{bmatrix} \\ \lambda^-(k) &= e^{-i(\alpha-1)kL} \end{aligned} \quad (40)$$

In the interval  $[\alpha^i L, \alpha^{i+1} L]$  the eigenvalue problem is

$$\begin{aligned} \frac{d^2 p}{dx^2} + k^2 p &= 0 \\ p(\alpha^{i+1} L) &= \lambda p(\alpha^i L) \\ q(\alpha^{i+1} L) &= \lambda q(\alpha^i L) \end{aligned} \quad (41)$$

and has the solutions

$$\begin{aligned} \Phi^{i+}(k) &= \begin{bmatrix} 1 \\ 1 \end{bmatrix} = \Phi^+(\alpha^i k) \\ \Psi^{i+}(k) &= \begin{bmatrix} \frac{1}{2} & \frac{1}{2} \end{bmatrix} = \Psi^+(\alpha^i k) \\ \lambda^{i+}(k) &= e^{i(\alpha-1)\alpha^i kL} = \lambda^+(\alpha^i k) \\ \Phi^{i-}(k) &= \begin{bmatrix} 1 \\ -1 \end{bmatrix} = \Phi^-(\alpha^i k) \\ \Psi^{i-}(k) &= \begin{bmatrix} \frac{1}{2} & -\frac{1}{2} \end{bmatrix} = \Psi^-(\alpha^i k) \\ \lambda^{i-}(k) &= e^{-i(\alpha-1)\alpha^i kL} = \lambda^-(\alpha^i k) \end{aligned} \quad (42)$$

In this case relation (42) yields  $\Psi^0(\alpha^i k)\Phi^0(\alpha^{i-1} k) = \mathbf{I}$ , and relation (33) leads finally to

$$\mathbf{s}^n = \Phi^{n-1} \Lambda^{n-1} \dots \Lambda^0 \Psi^0 \mathbf{s}^0 \quad (43)$$

and the amplitudes of waves are

$$\mathbf{a}^n = \Lambda^{n-1} \dots \Lambda^0 \mathbf{a}^0 \quad (44)$$

As the incoming waves should have null amplitudes at infinity, the final relation is  $\mathbf{a}^{n-} = 0$ , which can also be written in this simple case as (see also relation (37))

$$\Psi_p^{0-} p^0 + \Psi_q^{0-} q^0 = 0 \quad (45)$$

Here  $\Psi_p^{0-} = \frac{1}{2}$  is the first component of vector  $\Psi^{0-}$  and  $\Psi_q^{0-} = -\frac{1}{2}$  is the second component. So the final relation is

$$q^0 = -(\Psi_q^{0-})^{-1} \Psi_p^{0-} p^0 \quad (46)$$

In the present case, this yields

$$p'(L) = ikp(L) \quad (47)$$

which is the usual Sommerfeld condition.

#### 3.2 Acoustic waves in an annular domain

##### 3.2.1 Equations in an annular domain

Consider an annular circular domain with the internal radius  $r_i$  and the external radius  $r_e$ . This domain is exterior to the surface of a circular body  $\Omega$ . We are looking for the pressure  $p$ , solution of the eigenvalue problem

$$\begin{aligned} \Delta p + k^2 p &= 0 \\ \sqrt{r_e} p_e &= \lambda \sqrt{r_i} p_i \\ \frac{\sqrt{r_e}}{ik} \frac{\partial p_e}{\partial r} &= \lambda \frac{\sqrt{r_i}}{ik} \frac{\partial p_i}{\partial r} \end{aligned} \quad (48)$$

where  $p_i, p_e$  are the internal and external values of the pressure  $p$  and  $\lambda$  the eigenvalue. The state vector is defined as

$$\mathbf{s}(r) = \begin{bmatrix} \sqrt{r} p(r, \theta) \\ \frac{\sqrt{r}}{ik} \frac{\partial p}{\partial r}(r, \theta) \end{bmatrix} \quad (49)$$

and so is made of a first component proportional to the pressure and a second component proportional to the velocity.

The solution of the partial differential equation in the annular domain is given by

$$p(r, \theta) = \sum_{n=-\infty}^{\infty} (a_n H_n^1(kr) + b_n H_n^2(kr)) e^{in\theta} \quad (50)$$

where  $a_n, b_n$  are complex coefficients and  $H_n^1$  and  $H_n^2$  are Hankel functions of order  $n$  of first and second types respectively.

The eigenvalue problem (48) can be written as

$$\begin{vmatrix} \sqrt{r_e} H_n^1(kr_e) - \lambda \sqrt{r_i} H_n^1(kr_i) & \sqrt{r_e} H_n^2(kr_e) - \lambda \sqrt{r_i} H_n^2(kr_i) \\ \sqrt{r_e} \frac{\partial}{\partial r} H_n^1(kr_e) - \lambda \sqrt{r_i} \frac{\partial}{\partial r} H_n^1(kr_i) & \sqrt{r_e} \frac{\partial}{\partial r} H_n^2(kr_e) - \lambda \sqrt{r_i} \frac{\partial}{\partial r} H_n^2(kr_i) \end{vmatrix} = 0 \quad (51)$$

The determinant is the quadratic function of  $\lambda$

$$\begin{aligned} \lambda^2 + \frac{\pi k}{4i} \sqrt{r_i r_e} (H_n^1(kr_i) H_n^{2'}(kr_e) + H_n^1(kr_e) H_n^{2'}(kr_i) \\ - H_n^2(kr_i) H_n^{1'}(kr_e) - H_n^2(kr_e) H_n^{1'}(kr_i)) \lambda + 1 = 0 \end{aligned} \quad (52)$$

It can be seen that the eigenvalues come in inverse pairs  $\lambda_n$  and  $1/\lambda_n$ . Denoting by  $\Phi_n^+$  and  $\Phi_n^-$  the eigenvectors respectively associated to  $\lambda_n$  and  $1/\lambda_n$ , the solutions of equation (52) lead to the decomposition

$$s(r_i) = \left[ \frac{\sqrt{r_i} p(r_i, \theta)}{ik \frac{\partial p}{\partial r}(r_i, \theta)} \right] = \sum_{n=-\infty}^{\infty} (a_n^+ \Phi_n^+(r_i) + a_n^- \Phi_n^-(r_i)) e^{in\theta} \tag{53}$$

with the eigenvectors given by

$$\Phi_n^+(r_i) = \begin{bmatrix} \{ -(\sqrt{r_e} H_n^2(kr_e) - \lambda_n \sqrt{r_i} H_n^2(kr_i)) \sqrt{r_i} H_n^1(kr_i) \\ + (\sqrt{r_e} H_n^1(kr_e) - \lambda_n \sqrt{r_i} H_n^1(kr_i)) \sqrt{r_i} H_n^2(kr_i) \} \\ \frac{1}{ik} \{ -(\sqrt{r_e} H_n^2(kr_e) - \lambda_n \sqrt{r_i} H_n^2(kr_i)) \sqrt{r_i} \frac{\partial}{\partial r} H_n^1(kr_i) \\ + (\sqrt{r_e} H_n^1(kr_e) - \lambda_n \sqrt{r_i} H_n^1(kr_i)) \sqrt{r_i} \frac{\partial}{\partial r} H_n^2(kr_i) \} \end{bmatrix}$$

$$\Phi_n^-(r_i) = \begin{bmatrix} \{ -(\sqrt{r_e} H_n^2(kr_e) - \frac{1}{\lambda_n} \sqrt{r_i} H_n^2(kr_i)) \sqrt{r_i} H_n^1(kr_i) \\ + (\sqrt{r_e} H_n^1(kr_e) - \frac{1}{\lambda_n} \sqrt{r_i} H_n^1(kr_i)) \sqrt{r_i} H_n^2(kr_i) \} \\ \frac{1}{ik} \{ -(\sqrt{r_e} H_n^2(kr_e) - \frac{1}{\lambda_n} \sqrt{r_i} H_n^2(kr_i)) \sqrt{r_i} \frac{\partial}{\partial r} H_n^1(kr_i) \\ + (\sqrt{r_e} H_n^1(kr_e) - \frac{1}{\lambda_n} \sqrt{r_i} H_n^1(kr_i)) \sqrt{r_i} \frac{\partial}{\partial r} H_n^2(kr_i) \} \end{bmatrix} \tag{54}$$

To clarify the precedent relations, consider the case for large values of  $kr_i$  for which equation (52) simplifies to

$$\lambda^2 - 2\lambda \cos k(r_e - r_i) + 1 \approx 0 \tag{55}$$

and the eigenvalues are approximately

$$\lambda_n \approx e^{ik(r_e - r_i)} \tag{56}$$

$$1/\lambda_n \approx e^{-ik(r_e - r_i)} \tag{57}$$

as if the curvature of the boundary was neglected. The eigenvectors can be normalised to get

$$\Phi_n^+(r_i) \approx \begin{bmatrix} 1 \\ 1 \end{bmatrix}$$

$$\Phi_n^-(r_i) \approx \begin{bmatrix} 1 \\ -1 \end{bmatrix} \tag{58}$$

while

$$\Psi_n^+(r_i) \approx \frac{1}{2} \begin{bmatrix} 1 & 1 \end{bmatrix}$$

$$\Psi_n^-(r_i) \approx \frac{1}{2} \begin{bmatrix} 1 & -1 \end{bmatrix} \tag{59}$$

One gets

$$\Psi^0(\alpha^i k) \Phi^0(\alpha^{i-1} k) = \mathbf{I} \tag{60}$$

and following relation (33), the total matrix for  $N$  layers is

$$\mathbf{T}^{tot} = \begin{bmatrix} \Phi^{(N-1)+} & \Phi^{(N-1)-} \end{bmatrix} \begin{bmatrix} e^{ik(r_{N-1} - r_0)} & 0 \\ 0 & e^{-ik(r_{N-1} - r_0)} \end{bmatrix} \begin{bmatrix} \Psi^{0+} \\ \Psi^{0-} \end{bmatrix} \tag{61}$$

and relation (36) yields

$$\Psi^{0-} \mathbf{T}^{tot} = e^{-ik(r_{N-1} - r_0)} \Psi^{0-} \tag{62}$$

So the boundary condition is

$$\Psi^{0-} \mathbf{s}^0 = 0 \tag{63}$$

or

$$\sqrt{r} p - \frac{\sqrt{r}}{ik} \frac{\partial p}{\partial r} = 0 \tag{64}$$

We get the usual relation

$$\frac{\partial p}{\partial n} - ikp = 0 \tag{65}$$

### 3.2.2 Results for the annular domain

Some numerical values are computed, first for the pseudo wavenumber defined by  $K = \frac{\log \lambda}{i(r_e - r_i)}$ . A cylinder of radius  $r_i = 1m$  is considered with a sound velocity  $c = 343m/s$ . The first layer around the cylinder has a thickness of  $0.01m$ . Figure 3 present the real and imaginary parts of the wavenumber  $K$  versus the order  $n$  of the Hankel functions. It can be observed

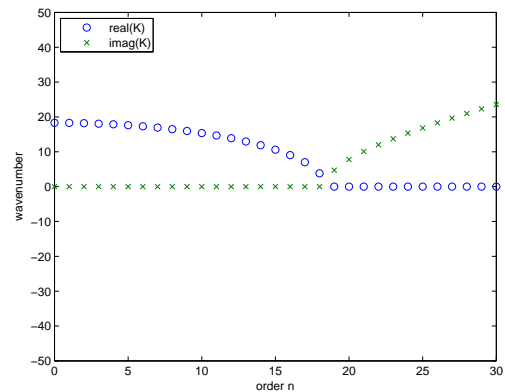
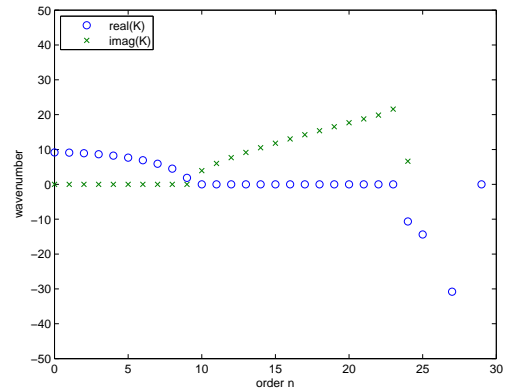


Figure 3. Wavenumbers for the frequency 500Hz (upper graph) and 1000Hz (lower graph).

that for low orders the wavenumber is real and becomes with an imaginary part when a critical order is reached. A higher frequency leads to more wavenumbers with purely real values. So it is analogous to classical waveguides with a cut-off frequency for which a given mode becomes propagative. Figure 4 presents the imaginary parts of the wavenumbers versus the frequency for different orders  $n$ . As long as the imaginary part of the wavenumber is null, the mode is propagating. It can be observed, for each mode, that the imaginary part becomes null when the frequency is higher than a critical frequency depending on the mode order.

Consider now axisymmetric problems (that means with only the zero order Hankel function). The boundary impedance,  $p/v$  at  $r_i$  is computed for the present method with relation (37) and compared to the analytical solution obtained with only the radiating Hankel function which equals  $-ipc \frac{H_0}{H_1}$ . Figure 5 presents the relative error for different numbers of layers. The computations are made with  $r_i = 1m$  and  $\alpha = 1.01$  ( $r_e = \alpha r_i$ ). It can be seen that a greater number of layers clearly improves

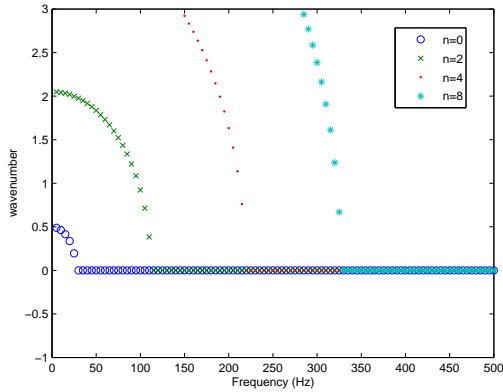


Figure 4. Imaginary part of the wavenumber for different orders.

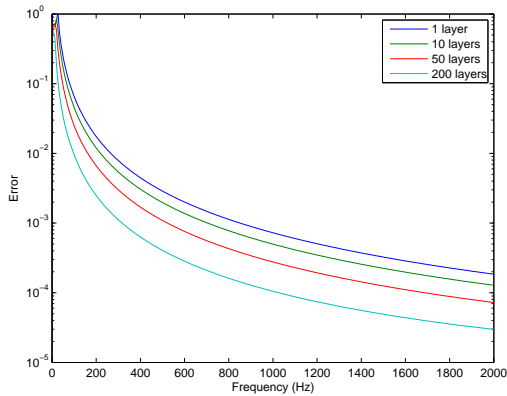


Figure 5. Error versus the number of layers.

the accuracy of the computation. Using only one layer can be sufficient except for very low frequencies.

### 3.3 Numerical examples

We present now some examples of radiation and scattering of acoustic waves by using the precedent numerical model.

#### 3.3.1 Surface impedance on a cylinder

Consider the case where an annular domain is meshed with one layer of four nodes linear acoustic elements. The cylinder is of radius  $1m$  and the sound velocity is  $c = 343m/s$ . The results present the error between the analytical impedance and the impedance found by the present method for the case of a uniform loading (independent of the direction). Three possible thicknesses are considered for the layer and the results are plotted in figure 6 for different numbers of elements in the mesh. It can be seen that interesting results can be obtained with only one layer and with a limited number of degrees of freedom. Increasing the mesh density leads to much better results except when the thickness of the layer and the frequency are so large that the error is mainly controlled by a too large thickness.

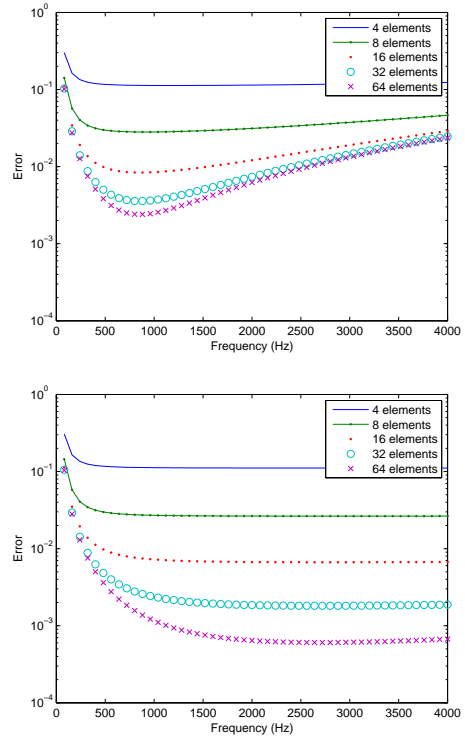


Figure 6. One layer with  $e = 0.01m$  (upper graph) and  $e = 0.001m$  (lower graph).

#### 3.3.2 Scattering by a cylinder

Consider now the problem of scattering of a point source by a rigid cylinder. The geometry is shown in figure 7. The cylinder

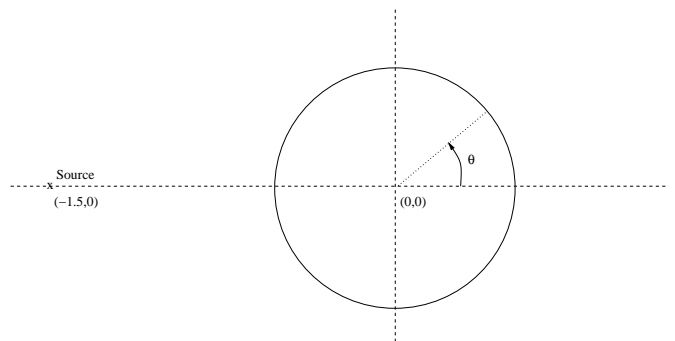


Figure 7. Geometry of the circle used in the computations.

has a radius of  $1m$  and the source is located at point  $(-1.5, 0)$ . The mesh is made of 128 elements of thickness  $0.005m$ . The problem is similar to the precedent example but the force  $\mathbf{f}_0$  is given by the nodal values of  $-\frac{1}{ik} \frac{\partial p_{inc}}{\partial n}$  where  $p_{inc}$  is the incident pressure. This incident pressure is given by  $\frac{i}{4} H_0(kr)$  where  $r$  is the distance between the source and the point of computation and  $H_0$  is the Hankel function of first type and order 0. The solution of the problem allows the computation of the scattering pressure and by adding the incident pressure, the total pressure is found around the cylinder. In figure 8, the pressure around the cylinder is computed for three different frequencies. The

results are presented versus the angle along the cylinder, the source being located in the direction with angle  $\pi$ .

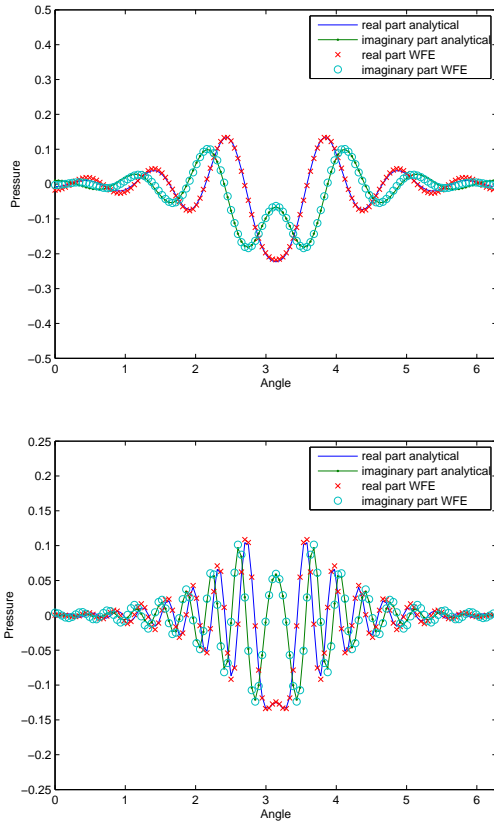


Figure 8. Pressure versus the angle along the cylinder for the frequencies 300Hz (upper graph) and 900Hz (lower graph) with a discretization of 128 elements.

The pressure is computed on the surface of the cylinder and the analytical values along with the numerical results are plotted for three frequencies. It can be observed a very good agreement at low frequencies. As the frequency increases, the error also increases.

#### 4 CONCLUSION

It has been shown that simple computations of eigenvalues and eigenvectors defined on a small rib around a radiating body for various frequencies could solve the problem of acoustic radiation in the complete exterior domain for any frequency as long as a sufficient number of layers or frequencies are involved in the computation. Tests on circular cases have provided accurate results. The approach has now to be extended to solve numerically cases with more complex geometries and non convex bodies.

#### REFERENCES

[1] J.B. Keller, D. Givoli, A finite element method for large domains, *Comput. Methods Appl. Mech. Engrg.*, 76 (1989) 41-66.  
 [2] P. Bettess, Infinite elements, *Int. J. Numer. Methods Engrg.*, 11 (1977) 53-64.  
 [3] J.P. Bérenger, A perfectly matched layer for the absorption of electromagnetic waves, *J. Comput. Physics*, 114 (1994) 185-200.

[4] B. Engquist, A. Majda, Absorbing boundary conditions for the numerical simulation of waves, *Mathematics of computation*, 31 (1977) 629-651.  
 [5] D. Duhamel, T.-M. Nguyen, Finite element computation of absorbing boundary conditions for time-harmonic wave problems, *Comput. Meth. Appl. Mech. and Eng.*, 198 (2009) 3006-3019.  
 [6] C.A. Brebbia, S. Walker, *Boundary elements techniques in engineering*, Newnes-butterworths, London, England, (1980).  
 [7] R.D. Ciskowski, C.A. Brebbia, *Boundary element methods in acoustics*, Computational mechanics publications, Elsevier, Southampton, England, (1991).  
 [8] M. Bonnet, *Boundary integral equation methods for solids and fluids*, Wiley, Chichester, England, (1995).  
 [9] V. Rokhlin, Rapid solution of integral equations of classical potential theory, *J. Comput. Phys.*, 60 (1985) 187-207.  
 [10] V. Rokhlin, Rapid solution of integral equations of scattering theory in two dimensions, *J. Comput. Phys.*, 86 (1990) 414-439.  
 [11] E. Darve, The fast multipole method: numerical implementation. *J. Comput. Phys.*, 160 (2000) 195-240.  
 [12] S. Finnveden, Evaluation of modal density and group velocity by a finite element method, *Journal of Sound and Vibration*, 273 (2004) 51-75.  
 [13] F. Birgersson, S. Finnveden and C.M. Nilsson, A spectral super element for modelling of plate vibration. Part 1: general theory, *Journal of Sound and Vibration*, 287 (2005) 297-314.  
 [14] S. Finnveden and M. Fraggstedt, Waveguide finite elements for curved structures, *Journal of Sound and Vibration*, 312 (2008) 644-671.  
 [15] I. Bartoli, A. Marzani, F. Lanza di Scalea and E. Viola, Modeling wave propagation in damped waveguides of arbitrary cross-section. *Journal of Sound and Vibration*, 295 (3-5) (2006) 685-707.  
 [16] L. Brillouin, *Wave propagation in periodic structures*, New York: Dover, (1953).  
 [17] D.J. Mead, *Wave propagation in continuous periodic structures: research contributions from Southampton, 1964-1995*, *Journal of Sound and Vibration*, 190 (1996) 495-524.  
 [18] D.J. Mead, A general theory of harmonic wave propagation in linear periodic systems with multiple coupling, *Journal of Sound and Vibration*, 27 (1973) 235-260.  
 [19] D.J. Mead, Wave propagation and natural modes in periodic systems: I. Mono-coupled systems, *Journal of Sound and Vibration*, 40 (1975) 1-18.  
 [20] D.J. Mead, Wave propagation and natural modes in periodic systems: II. Multi-coupled systems, with and without damping, *Journal of Sound and Vibration*, 40 (1975) 19-39.  
 [21] B.R. Mace, D. Duhamel, M.J. Brennan and L. Hinke, Finite element prediction of wave motion in structural waveguides, *Journal of the Acoustical Society of America*, 117 (2005) 2835-2843.  
 [22] J.M. Mencik and M.N. Ichchou, Multi-mode propagation and diffusion in structures through finite elements, *European Journal of Mechanics A/Solids*, 24 (2005) 877-898.  
 [23] L. Houillon, M.N. Ichchou and L. Jezequel, Wave motion in thin-walled structures, *Journal of Sound and Vibration*, 281 (2005) 483-507.  
 [24] Y. Waki, B.R. Mace, M.J. Brennan, Numerical issues concerning the wave and finite element method for free and forced vibrations of waveguides, *Journal of Sound and Vibration*, 327 (2009) 92-108.  
 [25] M.N. Ichchou, S. Akrouf, J.-M. Mencik, Guided waves group and energy velocities via finite elements, *Journal of Sound and Vibration*, 305 (2007) 931-944.  
 [26] D. Duhamel, B.R. Mace, M.J. Brennan, Finite element analysis of the vibrations of waveguides and periodic structures, *Journal of Sound and Vibration*, 294 (2006) 205-220.  
 [27] D. Duhamel, Finite element computation of Green's functions, *Engrg. Anal. Bound. Elem.*, 31 (2007) 919-930.